JETIR.ORG ISSN: 2349-5162 | ESTD Year : 2014 | Monthly Issue
JOURNAL OF EMERGING TECHNOLOGIES AND INNOVATIVE RESEARCH (JETIR)
An International Scholarly Open Access, Peer-reviewed, Refereed Journal

Texture and Frequency Based Medical Image Pulmonary Disease Prediction

Urvashi Dubey,Amar Nayak,Rajesh Boghey
Technocrats Institute of Technology,Execellence
Bhopal,M.P. India

***Abstract*—**Human life is important and many of researchers are working to develop better diagnosis models. Pulmonary disease infection are increasing hence easy detection and prediction algorithms are in demand. This paper has proposed a model TFFPDP that classify the input medical image (X-Ray) into infected and non-infected class. In order to increase the detection accuracy this work has utilized co-occurrence matrix model that extract texture feature from the image. Further Discrete Wavelet Transform model was used that extract frequency feature form the image. Both features were used for the training of convolutional neural network. Experiment was done on real dataset images and result shows that proposed model has improved the detection accuracy by 2.126% as compared to existing model of pulmonary disease detection.Further it was found that use of CNN model has increases the work f-measure value by 2.82% as compared to LFA-RNN .

Index Terms— Pulmonary Disease, Image Processing, Information Extraction, Visual Processing,Machine Learning.

I. INTRODUCTION

The forearm muscle known as palmarislongus aids in flexing the wrist. Although the Palmaris longus muscle is a common one in the human body, some persons may have a different type of it. In general, the Longissimus muscle itself is unaffected by any particular disorders. However, if there is an underlying ailment that affects the forearm or wrist, this muscle may be impacted [1]. The Palmaris longus muscle, among other tendons and muscles in the forearm and wrist, can be harmed by illnesses including carpal tunnel disease, tendonitis, or arthritis.

The following methods are used for the identification of pulmonary diseases:

Chest X-ray: The first test used to identify pulmonary illnesses, a chest X-ray can give a clear image of the lungs. It is capable of identifying anomalies such infections, lung cancer, or emphysema.

An enhanced imaging method that produces a three-dimensional view of the lungs is the CT scan. It can pick up on tiny anomalies like blood clots or lung infected that a chest X-ray would miss [2, 3].Testing the lungs' ability to function is known as a pulmonary function test, or PFT. They can aid in the diagnosis of diseases such pulmonary fibrosis, chronic obstructive pulmonary disease (COPD), and asthma [4]. A bronchoscopy is a method that allows a clinician to inspect the lungs' inside and collect lung tissue samples for testing. It is frequently employed to identify infections or lung cancer.

Techniques for machine learning can help identify and diagnose lung illnesses. Among the often employed machine learning methods for detecting pulmonary diseases are:

CNNs are a sort of deep learning algorithm that can be used to evaluate medical pictures like chest X-rays or CT scans [5]. Doctors may be able to identify patterns and irregularities in the images that could be signs of respiratory conditions such pneumonia, lung cancer, or tuberculosis.Support vector machines (SVMs) are a sort of supervised learning algorithm that are useful for categorising data. They can be used to categorise medical information into various disease categories, such as the results of blood tests or pulmonary function tests. Gaussian process models: These probabilistic models can be used to examine time-series data, such as the outcomes of pulmonary function tests over time[6]. They can be applied to forecast illness development and evaluate the effectiveness of treatments.

This paper proposed a neural network based pulmonary diseae prediction model. Rest of paer was organized into few section where second section includes related work done for disease prediction. Third section brief whole TFFPDP model. Experimental section justify the work outcome with comparison of existing method on various evaluation parameters. Finally work was concluded.

III. Related Work

By training primarily on chest X-ray data from healthy people, K. S. Kim et al. [7] suggested a deep-learning-based diagnostic system termed contrast-shifted instances via patch-based percentile (CSIP) to accurately discover pathological lung shadowing. The CSIP project is the first attempt to apply a patch-based percentile technique to modern one-class classifiers (OCCs).

The suggested approach by H. C. Kuo et al. in [8] successfully uses canonical correlation analysis to identify wheezing characteristics in a lung sound spectrogram. Also, a neural network approach is used to distinguish between wheezing and healthy noises.

A unique deep generative model known as a class activation region influence maximisation conditional adversarial network with generative capabilities was proposed by K. Ann et al. in [9]. (CARIM-cGAN). Using a programmable conditional mask, the suggested network can regulate the size, location, and presence of the target disease. To increase the likelihood of disease occurring in the confined region denoted by a conditional mask, we have developed class activation location influence maximisation (CARIM) loss. We performed a number of both quantitative and qualitative evaluations with the samples produced by a CARIM-cGAN to show an improved generating performance.

Alafif et al. [11] summarise the research on the application of ML and DL for COVID-19 diagnosis and therapy. The review study gives an overview of the AI-based ML and DL techniques, the datasets that are available, performance, and the tools that are now in use. Obstacles to completing the study can be overcome by doing a thorough examination of the current ML and DL methods used to diagnose COVID-19. The challenges in carrying out the investigations have been emphasised by completing a thorough study of the current ML and DL methods used to diagnose COVID-19. The report also provided some recommendations for future research. Several viewpoints on the likely interaction of ML, DL, and the COVID-19 virus were not explored, despite the fact that the study exclusively examined the usage of ML and DL techniques for the detection and management of COVID-19.

Alballa et alreview's of current articles on ML techniques used to the COVID-19 pandemic [11] was conducted. The study examined the uses of ML for diagnosing patients and estimating the likelihood and severity of patient mortality. Studies released during January 2020 and January 2021 are included in the review. A small amount of live E2E systems and a bias in selection brought on by uneven data were discovered by evaluating the investigations. Although the ML models have been examined for prediction and identification, other COVID-19-related goals like detection, epidemic prediction, etc. have not been taken into account.

In their [12] study, Alqudah, A.M. et al. assessed three distinct deep learning models on both non-enhanced and augmented datasets, using two different datasets to produce four different sub-datasets. The findings demonstrate that all of the deep learning techniques put forth were effective and produced good performance when it came to categorising the raw lung sounds. The techniques were used on various datasets and either used augmentation or did not. The CNN-LSTM model was the most effective deep learning model across all datasets for both enhancement and non-augmentation instances. The deep learning models' performance on the given workload is significantly improved with the help of the augmentation process.

III. Proposed Methodology

In this section proposed model TFFPDP (Texture and Frequency Feature based Pulmonary Disease Prediction) was detailed. Whole work was divided into two modules. First module work on image pre-processing steps, after this CCM and DCT feature extraction. Second module learns the extracted features from the image. Various steps of proposed model was shown in fig. 1.

Input Image Preprocessing

The input medical image IMI, dataset underwent preliminary processing to lower the model's operating expenses and noise levels. The image was converted into a square matrix known as Medical Image (MI) during pre-processing [13]. Also, this research identifies the portion of the picture that contains leaves separate from the background [14]. While the input image was in RGB format, the selected region was converted to HSV and Gray format.

MI←Pre-Processing(IMI)

CCM

The leaf texture element is crucial for identifying the image's heath. Red, Green, Hue, and Saturation matrix values were taken into consideration while the image was converted to RGB and HSV format [15]. The Modified Co-Occurrence Matrix (MCCM) feature is extracted from the image in this paper. Several of the negative and low values are deleted from the CCM feature set (Energy, Entropy, Inverse Difference, and Contrast). This updated value set is a CCM model modification. It was discovered that MCCM learning of the models was highly utilized. Four elements—contrast, energy, inverse difference, and entropy—were picked for this paper.

$$ID = \sum_{i=1}^{m}\sum_{j=1}^{n}\frac{1}{(1+(i-j)^2)}MI(i,j)$$

where PI(i, j) the intensity value in cell (i, j).

$$Entropy = \sum_{i=1}^{m}\sum_{j=1}^{n}MI(i,j)\log(MI(i,j))$$

$$Energy = \sum_{i=1}^{m}\sum_{j=1}^{n}MI(i,j)^2$$

$$Contrast = \sum_{i=1}^{m}\sum_{j=1}^{n}(i,j)^2 MI(i,j)$$

DWT (Discrete Wavelet Transform)

In this work DWT frequency feature was used. Here fig. 2 shows detail steps of DWT where work has embedded watermark in LL region of the image [16, 17]. This block of image is obtain by filtering the image rows from the low pass filter then pass same to the low pass filter but here column are filter for the analysis. This block contain flat region of the image which do not have any edge information, so this is term as approximate version of the image [18].

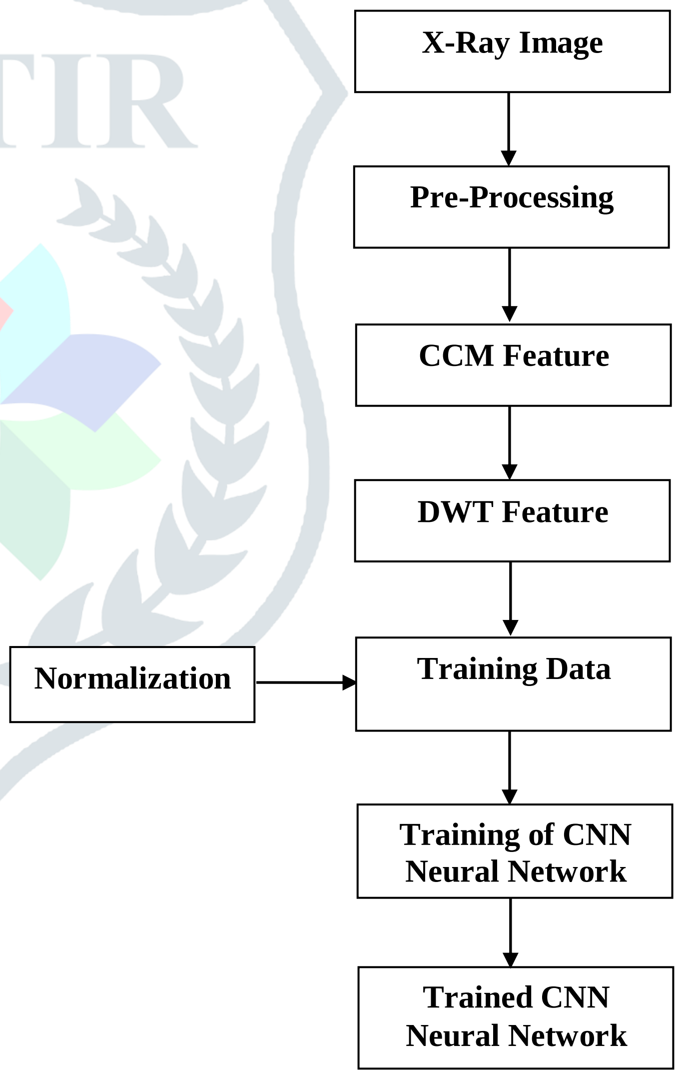

Fig. 1 Block diagram of TFFPDP model.

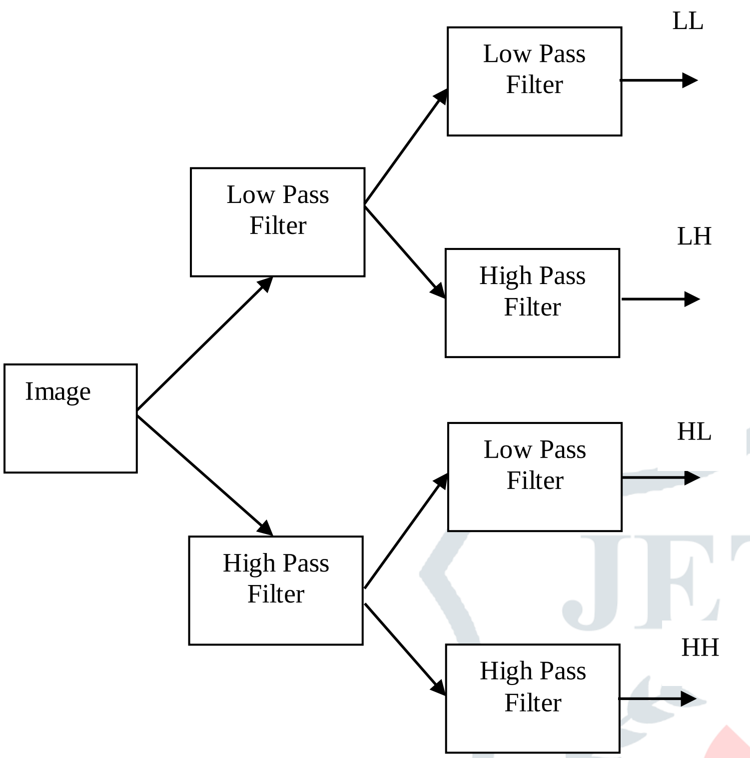

Fig. 2 DWT of lena image from [8].

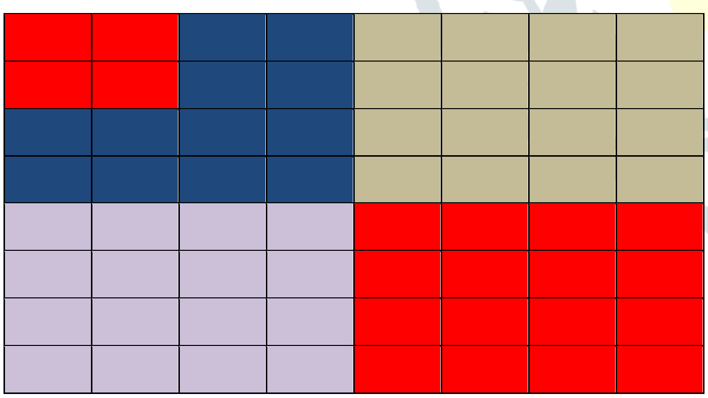

Convolutional Neural Network Training:

Convolutional processing. The network should be able to extract position-invariant image features. Hence, using various weights for different portions of the image in the neural network is generally not necessary. As a result, the convolution operation in CNNs applies a tiny convolution mask to the 2D input. The convolution process has two key benefits. (1) Image data maintains its 2D structure. Convolution-based extraction of features is therefore superior to fully connected operation in terms of effectiveness. (2) It significantly reduces the number of unknown parameters in the network because various picture portions share the same weight parameters. CNNs are therefore simpler to train and less prone to over-fitting [19].

$$C \leftarrow \text{Convolution}(CCM, DWT, s, p, F)$$

Stride s is an integer-valued movement speed control variable. If necessary, add a row or column to the block with padding of null. F applies a filter to the matrix of CCM and DWT features.

Stride is movement speed control variable having integer values. Padding is null row or column add in the block if required. F is filter apply to the matrix.Convolution safeguards the spatial connection between pixels by learning picture features utilizing small squares of information.

$$B = \begin{vmatrix} 1 & 1 & 1 & 0 & 0 \\ 0 & 1 & 1 & 1 & 0 \\ 0 & 0 & 1 & 1 & 1 \\ 0 & 0 & 1 & 1 & 0 \\ 0 & 1 & 1 & 0 & 0 \end{vmatrix}$$

$$F = \begin{vmatrix} 1 & 0 & 1 \\ 0 & 1 & 0 \\ 1 & 0 & 1 \end{vmatrix}$$

Slide the selected grid over input picture by 1 pixel called 'stride' speak to as s and for each position, calculate matrix wise duplication and add the multiplication yield to get the final number which shapes a single component of the yield matrix. Note that the 3×3 matrix F act as filter or kernel, where size of filter depends on k. In this case padding value p=0 is consider.

$$\begin{vmatrix} 1 & 1 & 1 & 0 & 0 \\ 0 & 1 & 1 & 1 & 0 \\ 0 & 0 & 1 & 1 & 1 \\ 0 & 0 & 1 & 1 & 0 \\ 0 & 1 & 1 & 0 & 0 \end{vmatrix} X \begin{vmatrix} 1 & 0 & 1 \\ 0 & 1 & 0 \\ 1 & 0 & 1 \end{vmatrix} = \begin{vmatrix} 4 & 3 & 4 \\ 2 & 4 & 3 \\ 2 & 3 & 4 \end{vmatrix}$$

Max-pooling

The receptive field of the extracted image features must be sufficiently large to accommodate items of varied sizes since the objects in the images may be of varying sizes (for example, huge infecteds and small infecteds). The primary idea behind it is to downscale the image feature maps in order to increase the receptive field. This downsampling in CNNs is typically accomplished through maximal pooling or average pooling. The convolution technique is s times more effective at enlarging the receptive field after multiplying the image feature maps by a factor of a. The pooling procedures often employ s = 2, and the convolution operations and the pooling operations frequently collaborate in groups to gradually encode high-level image information (from low-level to high-level).

$$C \leftarrow \text{Maxpooling}\ (CCM, DWT, s, p, F_m)$$

Practically speaking, Max Pooling has been appeared to work better. Here shifting was done as per stride value s and padding will be done as per p value.

$$\begin{vmatrix} 1 & 1 & 2 & 4 \\ 5 & 6 & 7 & 8 \\ 3 & 2 & 1 & 0 \\ 1 & 2 & 3 & 4 \end{vmatrix} \rightarrow \begin{vmatrix} 6 & 8 \\ 3 & 4 \end{vmatrix}$$

In above matrix let k=2, so window of 2x2 move around the image block. While s=1 and p=0.

Fully Convolutional Networks (FCN)

CNNs can use the spatial data provided in the input space with the help of convolution and pooling operations, but the per-pixel categorization formulation precludes the network from using the spatial correlation in the output space. Fully convolutional networks (FCNs) [20] were suggested as a solution to this issue. FCNs directly output the segmentation of the full input image rather than computing the classes of the pixels one at a time. Convolution and pooling operations preserve the picture structure in every hidden layer before fully linked processes, and these hidden feature maps contain entire information for every pixel in the image, as you can see. The target output was an infected or non-infected class and the input features generated after convolutional operation were supplied as the training vector in FCN. When given a processed (convolutional operation) features of image, a trained CNN will predict the block class (infected or non infected).

Proposed TFFPDP Algorithm

Input: PID // Pulmonary Image Dataset

Output: EPDM // Expert Pulmonary Detection Model

1. Loop 1:n
2. MI[n]←Image-Processing(PID[n])
3. CCM[n]←CCM_Feature_Extraction(MI[n])
4. [LL, LH, HL, HH]←DWT_Feature_Extraction(MI[n])
5. DWT[n]←LL
6. EndLoop
7. Loop 1:n
8. CF←Convolution(CCM[n], DWT[n]) // CF: Convolution Feature
9. CF[n]←maxpooling(CF)
10. EndLoop
11. CNN←Intialize_CNN()
12. Loop 1:Epoches
13. PDTM←TrainingCNN(CF, CNN)
14. EndLoop

IV. Evaluation Parameters

Experimental work was done on MATLAB and real dataset was taken form [21]. Comparison of proposed model was done with existing model proposed in [22].

Table 1 Sample dataset images.

Infected Images	Healthy Images
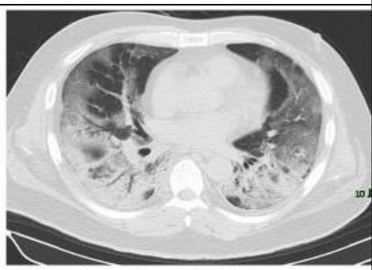	
	
	
	

Evaluation Parameters

In order to evaluate results there are many parameter such as accuracy, precision, recall, F-score, etc. Obtaining values can be put in the mention parameter formula to get results [17].

Precision =(True_Positive)/(True_Positive+ False_Positive)

Recall =(True_Positive)/(True_Positive+ False_Negative)

F-Measure =(2* Precision*Recall)/(Precision + Recall)

Accuracy =(True_Positive+ True_Negative)/(True_Positive+ True_Negative + False_Positive +False_Negative)

Results

Table 2. Pulmonary disease precision value based comparison.

Testing Dataset Size	LFA-RNN	TFFPDP
20+20	0.8844	0.95
30+30	0.8466	0.9333
40+40	0.88	0.95
50+50	0.8971	0.96
60+60	0.8801	0.9655

Precision values of pulmonary disease detection model was shown in table 2. It was found that proposed model has increases the true positive count of infected disease at various testing dataset images. Table 2 shows that precision values of pulmonary disease detection was improved by 7.78% as compared to existing model proposed in [].

Table 3. Pulmonary disease recall value based comparison.

Testing Dataset Size	LFA-RNN	TFFPDP
20+20	1	1
30+30	1	1
40+40	1	1
50+50	1	0.9744
60+60	1	0.9492

Recall values of pulmonary disease prediction models shown in table 3. It was found that use of CCM feature has perfectly identify the healthy images.

Table 4. Pulmonary disease f-measure value based comparison.

Testing Dataset Size	LFA-RNN	TFFPDP
20+20	0.9386	0.9744
30+30	0.9169	0.9655
40+40	0.9363	0.962
50+50	0.9458	0.9505
60+60	0.9362	0.9573

Inverse average of precision and recall values were shown in table 4. It was found that useof CCM and DWT feature for the training of the model has increases the work f-measure value by 2.82% as compared to LFA-RNN [].

Table 5. Pulmonary disease accuracy value based comparison.

Testing Dataset Size	LFA-RNN	TFFPDP
20+20	94.2111	96.4276
30+30	92.3240	96.6662
40+40	94.0056	96.2496
50+50	94.8555	94.9996
60+60	94.0049	95.6894

Correct class prediction of pulmonary disease detection models were shown in table 5 and it was found that use of CCM texture feature with frequency DWT feature has increases the work performance.

V. Conclusion

Technology reduces the load of various sector, but in heath diagnosis is still dependent on medical practioners. Load should be reduce by use of some prediction models. This paper has address same issue and proposed a model that identify the pulmonary infection from the X-ray images, without any patient background information. Proposed work extract CCM and DWT feature form the input image for the prediction of infected/non-infected class. Neural network was used for training of extracted features. Experiment was done on real dataset and result shows that use of CCM, DWT and neural has improved the work evaluation parameter values. Result shows that precision value of proposed TFFPDP model was improved by 7.78%, f-measure by 2.82% as compared to LFA-RNN model. Proposed TFFPDP modle accuracy of detection was enhanced by 2.126%.In future scholar can develop a new feature learning model.

References

1. Bradley, S.H.; Kennedy, M.; Neal, R.D. Recognizing lung cancer in primary care. Adv. Ther. 2019, 36, 19–30.
2. Athey, V.L.; Walters, S.J.; Rogers, T.K. Symptoms at lung cancer diagnosis are associated with major differences in prognosis. Thorax 2018, 73, 1177–1181.
3. Duma, N.; Santana-Davila, R.; Molina, J.R. Non–small cell lung cancer: Epidemiology, screening, diagnosis, and treatment. In Mayo Clinic Proceedings; Elsevier: Amsterdam, The Netherlands, 2019; Volume 94, pp. 1623–1640.
4. Romaszko, A.M.; Doboszyńska, A. Multiple primary lung cancer: A literature review. Adv. Clin. Exp. Med. 2018, 27, 725–730.
5. No Tobacco '22. Available online: https://www.lung.org/media/press-releases/no-tobacco-%E2%80%9922 (accessed on 6 August 2022).
6. S. Swaminathan, K. Qirko, T. Smith, E. Corcoran, N.G. Wysham, G. Bazaz, G. Kappel, A.N. Gerber A machine learning approach to triaging patients with chronic obstructive pulmonary disease PLoS One, 12 (11) (2017), Article e0188532
7. K. S. Kim, S. J. Oh, H. B. Cho and M. J. Chung, "One-Class Classifier for Chest X-Ray Anomaly Detection via Contrastive Patch-Based Percentile," in IEEE Access, vol. 9, pp. 168496-168510, 2021.
8. H. C. Kuo, B. -S. Lin, Y. -D. Wang and B. -S. Lin, "Development of Automatic Wheeze Detection Algorithm for Children With Asthma," in IEEE Access, vol. 9, pp. 126882-126890, 2021.

9. K. Ann, Y. Jang, H. Shim and H. -J. Chang, "Multi-Scale Conditional Generative Adversarial Network for Small-Sized Lung Nodules Using Class Activation Region Influence Maximization," in IEEE Access, vol. 9, pp. 139426-139437, 2021, doi: 10.1109/ACCESS.2021.

10. N. Alballa, I. Al-Turaiki Machine learning approaches in COVID-19 diagnosis, mortality, and severity risk prediction: a review Inform Med Unlocked, 24, 2021.

11. T. Alafif, A.M. Tehame, S. Bajaba, A. Barnawi, S. Zia Machine and deep learning towards COVID-19 diagnosis and treatment: survey, challenges, and future directions IJERPH, 18 (3) (2021).

12. Alqudah, A.M., Qazan, S. &Obeidat, Y.M. Deep learning models for detecting respiratory pathologies from raw lung auscultation sounds. Soft Comput 26, 13405–13429 (2022).

13. Abu SarwarZamani, L. Anand, KantilalPitambarRane, P. Prabhu, Ahmed MateenButtar, HarikumarPallathadka, AbhishekRaghuvanshi, Betty NokobiDugbakie, "Performance of Machine Learning and Image Processing in Plant Leaf Disease Detection", Journal of Food Quality, vol. 2022.
14. Chandan Kumar, Amit Kumar Singh, Pardeep Kumar. “A recent survey on image watermarking techniques and its application in e-governance”. Multimedia Tools and ApplicationsFebruary 2018, Volume 77, Issue 3 pp 3597–3622.
15. Shalinee Jain, Asst. Prof. SachinMalviya. "Digital Image Retrieval Using Annotation, CCM and Histogram Features". IJSRET, volume 4 issue 5, 2018.
16. Yicheng Sun, Xiubao Sui, GuohuaGu, Yuan Liu, ShuangshuangXu. “Compressive Super-Resolution Imaging Based on Scrambled Block Hadamard Ensemble”. IEEE Photonic Journal, Volume 8, Number 2, April 2016, 1943-0655.
17. P. Dabas and K. Khanna, “A study on spatial and transform domain watermarking techniques,” International Journal of Computer Applications, vol. 71, no. 14, pp. 38–41, 2013.
18. A. Al-Ataby, W. Al-Nuaimy, and M. A. M. Abdullah, Wavelet Transform-Multidisciplinary Applications. InTech, 2012, pp. 255–250.

19. C. Baur, S. Albarqouni, and N. Navab. Semi-supervised deep learning for fully convolutional networks. In International Conference on Medical Image Comput-ing and Computer-Assisted Intervention, pages 31-319, 2017.

20. J. Chen, L. Yang, Y. Zhang, M. Alber, and D. Z. Chen. Combining fully con-volutional and recurrent neural networks for 3D biomedical image segmentation. In Advances in Neural Information Processing Systems, pages 3036-3044, 2016.
21. https://github.com/UCSD-AI4H/COVID-CT/tree/master/Images-processed
22. C. -M. Kim, E. J. Hong and R. C. Park, "Chest X-Ray Outlier Detection Model Using Dimension Reduction and Edge Detection," in IEEE Access, vol. 9, pp. 86096-86106, 2021.